

INFLAMMATION

Familial autoinflammation with neutrophilic dermatosis reveals a regulatory mechanism of pyrin activation

Seth L. Masters,^{1,2*} Vasiliki Lagou,^{3,4,5†} Isabelle Jéru,^{6,7,8†} Paul J. Baker,^{1,2†} Lien Van Eyck,^{4,5} David A. Parry,⁹ Dylan Lawless,¹⁰ Dominic De Nardo,^{1,2} Josselyn E. Garcia-Perez,^{4,5} Laura F. Dagley,^{1,2,11} Caroline L. Holley,¹² James Dooley,^{4,5} Fiona Moghaddas,^{1,2} Emanuela Pasciuto,^{4,5} Pierre-Yves Jeandel,¹³ Raf Sciôt,^{14,15} Dena Lyras,¹⁶ Andrew I. Webb,^{2,11} Sandra E. Nicholson,^{1,2} Lien De Somer,¹⁵ Erika van Nieuwenhove,^{4,5,15} Julia Ruuth-Praz,^{7,8} Bruno Copin,⁸ Emmanuelle Cochet,⁸ Myrna Medlej-Hashim,¹⁷ Andre Megarbane,¹⁸ Kate Schroder,¹² Sinisa Savic,^{19,20} An Goris,³ Serge Amselem,^{6,7,8} Carine Wouters,^{4,15*‡} Adrian Liston^{4,5*‡}

Pyrin responds to pathogen signals and loss of cellular homeostasis by forming an inflammasome complex that drives the cleavage and secretion of interleukin-1 β (IL-1 β). Mutations in the B30.2/SPRY domain cause pathogen-independent activation of pyrin and are responsible for the autoinflammatory disease familial Mediterranean fever (FMF). We studied a family with a dominantly inherited autoinflammatory disease, distinct from FMF, characterized by childhood-onset recurrent episodes of neutrophilic dermatosis, fever, elevated acute-phase reactants, arthralgia, and myalgia/myositis. The disease was caused by a mutation in *MEFV*, the gene encoding pyrin (S242R). The mutation results in the loss of a 14-3-3 binding motif at phosphorylated S242, which was not perturbed by FMF mutations in the B30.2/SPRY domain. However, loss of both S242 phosphorylation and 14-3-3 binding was observed for bacterial effectors that activate the pyrin inflammasome, such as *Clostridium difficile* toxin B (TcdB). The S242R mutation thus recapitulated the effect of pathogen sensing, triggering inflammasome activation and IL-1 β production. Successful therapy targeting IL-1 β has been initiated in one patient, resolving pyrin-associated autoinflammation with neutrophilic dermatosis. This disease provides evidence that a guard-like mechanism of pyrin regulation, originally identified for Nod-like receptors in plant innate immunity, also exists in humans.

INTRODUCTION

Autoinflammatory diseases are characterized by recurrent episodes of fever with systemic and organ-specific inflammation, as well as uncontrolled activation of the innate immune response in the apparent absence

of an infectious trigger (1). Familial Mediterranean fever (FMF, OMIM ID: 249100) is the most common of the monogenic autoinflammatory diseases, characterized by short (24 to 72 hours) episodes of fever associated with serositis, progressing to amyloidosis if untreated (2). FMF is an autosomal recessive disease caused by mutations in both alleles of the *MEFV* (*Mediterranean fever*) locus, which encodes the protein pyrin (3, 4). Normally, pyrin functions as an innate immune sensor that can trigger formation of an inflammasome, allowing the production of inflammatory mediators during infection. Pyrin activation is mediated by oligomerization via the central BCC (B-box and coiled-coil) domain, which results in signaling through the N-terminal PYD (pyrin) domain to the inflammasome. Studies in mice indicate that FMF mutations are a gain of function (5); however, it is unclear how FMF mutations, typically in the C-terminal B30.2/SPRY domain, initiate the activation process. As a potent checkpoint for the initiation of inflammation, the molecular mechanisms of pyrin regulation are critical and yet still poorly understood.

RESULTS

We studied a three-generation Belgian family of 22 individuals, of whom 12 developed autoinflammatory disease (Fig. 1A). The disease was characterized by neutrophilic dermatosis, childhood-onset recurrent episodes of fever lasting several weeks, increased levels of acute-phase reactants, arthralgia, and myalgia/myositis (Fig. 1B). The neutrophilic dermatosis comprised a spectrum of clinical manifestations, including severe acne, sterile skin abscesses, pyoderma gangrenosum, and neutrophilic

¹Inflammation Division, The Walter and Eliza Hall Institute of Medical Research, Parkville, Victoria, 3052, Australia. ²Department of Medical Biology, The University of Melbourne, Parkville, Victoria 3010, Australia. ³Department of Neurosciences, KU Leuven, Leuven 3000, Belgium. ⁴Department of Microbiology and Immunology, KU Leuven, Leuven 3000, Belgium. ⁵Translational Immunology Laboratory, VIB, Leuven 3000, Belgium. ⁶INSERM, UMR S933, Paris F-75012, France. ⁷Université Pierre et Marie Curie–Paris, UMR S933, Paris F-75012, France. ⁸Assistance Publique Hôpitaux de Paris, Hôpital Trousseau, Service de Génétique et d'Embryologie médicales, Paris F-75012, France. ⁹Centre for Genomic and Experimental Medicine, Institute of Genetics and Molecular Medicine, University of Edinburgh, Western General Hospital, Crewe Road South, Edinburgh LS7 4SA, UK. ¹⁰Leeds Institute of Biomedical and Clinical Sciences, University of Leeds, Wellcome Trust Brenner Building, Saint James's University Hospital, Leeds LS7 4SA, UK. ¹¹Systems Biology and Personalised Medicine Division, The Walter and Eliza Hall Institute of Medical Research, Parkville, Victoria 3052, Australia. ¹²Institute for Molecular Bioscience (IMB) and IMB Centre for Inflammation and Disease Research, The University of Queensland, Brisbane, Queensland 4072, Australia. ¹³Département de Médecine Interne, Hôpital Archet 1, Université Nice Sophia-Antipolis, 06202 Nice, France. ¹⁴Department of Pathology, KU Leuven, Leuven 3000, Belgium. ¹⁵University Hospitals Leuven, Leuven 3000, Belgium. ¹⁶Department of Microbiology, Monash University, Melbourne, Victoria 3800, Australia. ¹⁷Department of Life and Earth Sciences, Faculty of Sciences II, Lebanese University, Beirut 1102 2801, Lebanon. ¹⁸Al-Jawhara Center, Arabian Gulf University, Manama 26671, Bahrain. ¹⁹Department of Allergy and Clinical Immunology, Saint James's University Hospital, Leeds LS9 7TF, UK. ²⁰National Institute for Health Research—Leeds Musculoskeletal Biomedical Research Unit and Leeds Institute of Rheumatic and Musculoskeletal Medicine, Wellcome Trust Brenner Building, Saint James's University Hospital, Beckett Street, Leeds LS9 7TF, UK.

*Corresponding author. E-mail: masters@wehi.edu.au (S.L.M.); carine.wouters@uzleuven.be (C.W.); adrian.liston@vib.be (A.L.)

†These authors contributed equally as second authors.

‡These authors contributed equally as co-last authors.

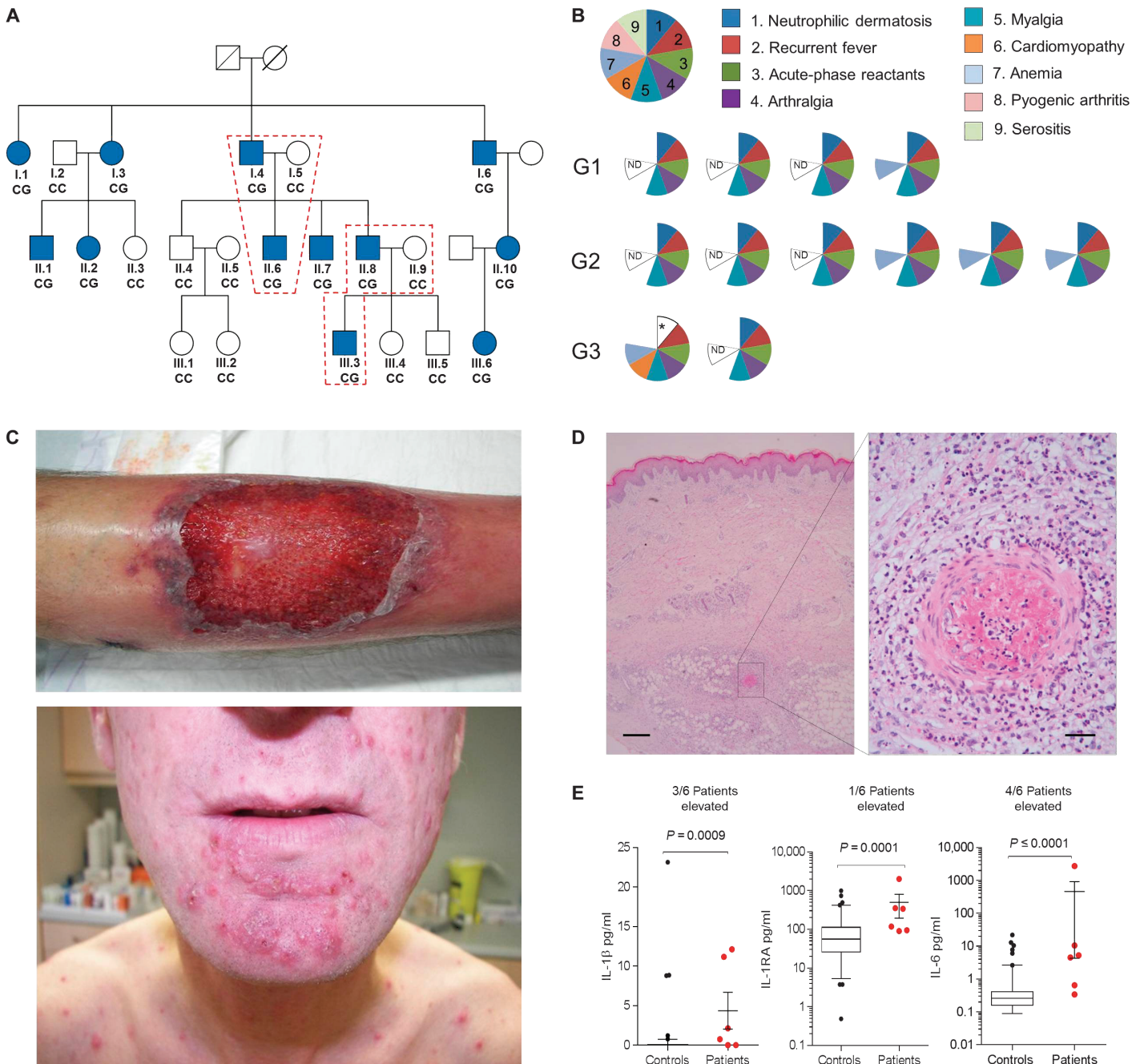


Fig. 1. Clinical and immunological features of PAAND. (A) Dominant inheritance of PAAND over three generations, with complete penetrance observed for the S242R mutation (*MEFV* c.C726G, denoted CG). Trios indicated by red boxing were subjected to exome sequencing. (B) Twenty-two family members were assessed for neutrophilic dermatosis, recurrent childhood-onset fever, acute-phase reactants, arthralgia, myalgia, cardiomyopathy, anemia, pyogenic arthritis, and serositis across three generations (G1, G2, and G3). ND, not determined; “*,” recent onset. (C) Typical macroscopic features (top: pyoderma lesions on the arm; bottom: pustular acne lesions on the face) (representative

small-vessel vasculitis (Fig. 1, C and D). Pathological examination of affected skin showed a dense, predominantly neutrophilic, vascular, perivascular, and interstitial infiltrate (Fig. 1D). Serum cytokine analysis

revealed elevated inflammatory mediators such as interleukin-1 β (IL-1 β), IL-6, and tumor necrosis factor- α (TNF- α) and cytokines induced by inflammation such as IL-1 receptor antagonist (IL-1Ra) (Fig. 1E and

fig. S1A). One patient (III.3) presented with additional dilated cardiomyopathy at 13 years of age, which evolved into chronic cardiac decompensation, necessitating cardiac transplantation at the age of 20 years. Analysis of a skeletal muscle biopsy from this patient indicated inflammatory infiltrate mainly composed of macrophages (fig. S1, B and C). Because of the genetic causation by pyrin mutation (see below) and the characteristic features of systemic inflammation and dermatosis, we termed this disease pyrin-associated autoinflammation with neutrophilic dermatosis (PAAND).

PAAND disease inheritance indicated a dominant mode of transmission (Fig. 1A). We therefore performed genome-wide linkage analysis on 20 family members, revealing a genome-wide significant LOD (logarithm of the odds ratio for linkage) score of 3.6 for a single region (1 to 6,283,321 on hg19) in chromosome 16 (fig. S2). Exome sequencing was performed on two linked trios within the pedigree (I.4, I.5, and II.6; II.8, II.9, and III.3), and we subjected the 8720 variants within the linkage region to our filtering pipeline, identifying a single synonymous variant in *RPL3L*, and a single missense mutation in *MEFV* (rs104895127) (fig. S3). Inheritance of this mutation was directly tested in the remaining members of the pedigree, displaying complete segregation with disease (Fig. 1A). The identified mutation was a C-to-G substitution at c.726 in exon 2 of *MEFV*, which results in a serine-to-arginine substitution at position 242 (S242R) in the pyrin protein. *MEFV* mutations are associated with the development of FMF; however, the S242R mutation falls in a protein region distinct from that of typical FMF-associated mutations (fig. S3). Some less common variants in *MEFV* have been reported near S242; however, their pathogenicity has not yet been evaluated. A few cases of dominantly inherited FMF have been reported in the literature (6–8); however, these are also not near S242R. Although not falling within a characterized protein domain, Ser²⁴² is highly conserved across mammals (fig. S3), unlike some of the more typical FMF variants that naturally occur in other species (9). Despite the association of *MEFV* mutations with FMF, the disease described here with S242R mutation is clinically distinct from FMF, with the absence of serositis and amyloidosis even after lifelong disease, the presence of severe recurrent neutrophilic dermatosis, and bouts of fever lasting several weeks rather than days (Fig. 1B). Clinical cutaneous manifestations evoked a closer resemblance to PAPA (pyogenic arthritis, pyoderma gangrenosum, and acne), which is caused by gain-of-function mutations in the pyrin-activating partner *PSTPIP1*, although here too it was distinct, with a lack of pyogenic arthritis (Fig. 1B).

To further investigate the physiological result of pyrin S242R mutation, we searched for other occurrences outside the investigated family. The variant was only seen in 1 of 122,836 chromosomes in 65000 Exome Aggregation Consortium (ExAC 65000) (allele frequency = 8×10^{-6}), in a Colombian male for whom clinical information was not available (1000 Genomes phase 1 database), and was absent in 1087 unrelated Belgian exomes [available on NGS-Logistics (10)]. Two other patients with the same mutation in *MEFV* had, however, been reported in the registry of mutations responsible for hereditary autoinflammatory diseases (InFevers, <http://fmf.igh.cnrs.fr/ISSAID/infevers/>) (11), and a third independent family was identified. The first was an individual from France with a heterozygous S242R mutation in the absence of any other coding *MEFV* mutations. Disease presentation was similar to the Belgian family, with recurrent inflammatory skin nodules associated with neutrophilic infiltrate and small-vessel vasculitis, fever, arthralgia/myalgia, and the absence of characteristic FMF symptoms, namely, serositis, and of amyloidosis (fig. S4A). The second individual was from Lebanon and

carried the S242R mutation in conjunction with a known FMF variant M694V. New clinical analysis was not possible; however, retrospective assessment of clinical manifestations included periodic fevers of 3- to 5-day duration and joint pain, partially controlled by colchicine treatment, as can be seen in FMF. Additional symptoms included recurrent aphthous ulcers, prompting an initial diagnosis of Behçet disease, chronically elevated C-reactive protein (CRP), and transient skin rashes/nodules (fig. S4B). A third independent family was identified in the UK and also demonstrated dominant inheritance of the PAAND phenotype (fig. S4C). Overall, the combination of inheritance in a pedigree exceptional by size and confirmation of the mutation in three additional pedigrees with autoinflammatory features strongly support the S242R mutation in pyrin as a causative driver of PAAND.

The unique clinical presentation of the S242R mutations suggested a distinct regulatory mechanism of pyrin-mediated activation of the inflammasome. Therefore, we analyzed ASC (apoptosis-associated speck-like protein containing a CARD) speck formation, which assembles as an intense cytoplasmic aggregate in response to pyrin activation (12). Green fluorescent protein (GFP)–ASC was overexpressed in human embryonic kidney (HEK) 293T cells at a level causing minimal spontaneous speck formation. With this system, the coexpression of pyrin colocalized with ASC and led to increased triggered speck formation, which was further enhanced by the S242R mutation (Fig. 2A and fig. S5, A and B). Quantification of ASC specks was performed by flow cytometry, using mCherry-tagged pyrin and further controlling for cells with similar expression levels of wild-type versus S242R pyrin (Fig. 2B and fig. S5C). The elevated speck formation of the S242R mutation was not observed from nearby heterozygous variants (R202Q and G304R) recently found in two Japanese patients who developed Sweet syndrome (Fig. 2C) (13). Typical FMF variants such as M680I and M694V did not lead to a significant increase in ASC specks in this assay; however, when double-mutant S242R/M694V pyrin was expressed, a significant increase was observed over the S242R single-mutant protein (Fig. 2C).

Downstream of ASC, the S242R mutation resulted in caspase-1 being activated, with increased production of the p20 subunit (Fig. 2D and fig. S6A) and incorporation into the inflammasome “speck” (fig. S6, B and C). To measure IL-1 β production, we used the human THP-1 monocytic cell line, with retroviral overexpression of wild-type or S242R pyrin. Lipopolysaccharide (LPS) was added for 24 hours to induce the synthesis of pro-IL-1 β , and a significant increase in mature, secreted IL-1 β was observed from cells expressing S242R pyrin compared to wild type (Fig. 2E and fig. S6D). This inflammasome activation was independent of NLRP3, as demonstrated by treatment with the NLRP3-specific inhibitor MCC950 (fig. S6E). CRISPR (clustered regularly interspaced short palindromic repeats)–mediated deletion of endogenous human pyrin (*MEFV*^{-/-}) confirms that loss-of-function mutation of pyrin does not trigger inflammasome activation and that endogenous pyrin was not required for pyrin S242R activation. By contrast, deletion of endogenous caspase-1 (*CASP1*^{-/-}) prevented IL-1 β production due to pyrin S242R (Fig. 2E). Another known consequence of increased caspase-1 activation is pyroptotic cell death, which was also increased by S242R expression (Fig. 2F).

To more closely examine the molecular mechanism by which S242R regulates pyrin activity, we immunoprecipitated glutathione S-transferase (GST)–tagged wild-type or S242R mutant protein from HEK293T cells. Eluates were run out on polyacrylamide gels and developed with a sensitive fluorescent protein stain, revealing a band that was specifically bound to the wild-type and not to the mutant protein (fig. S7A). Mass

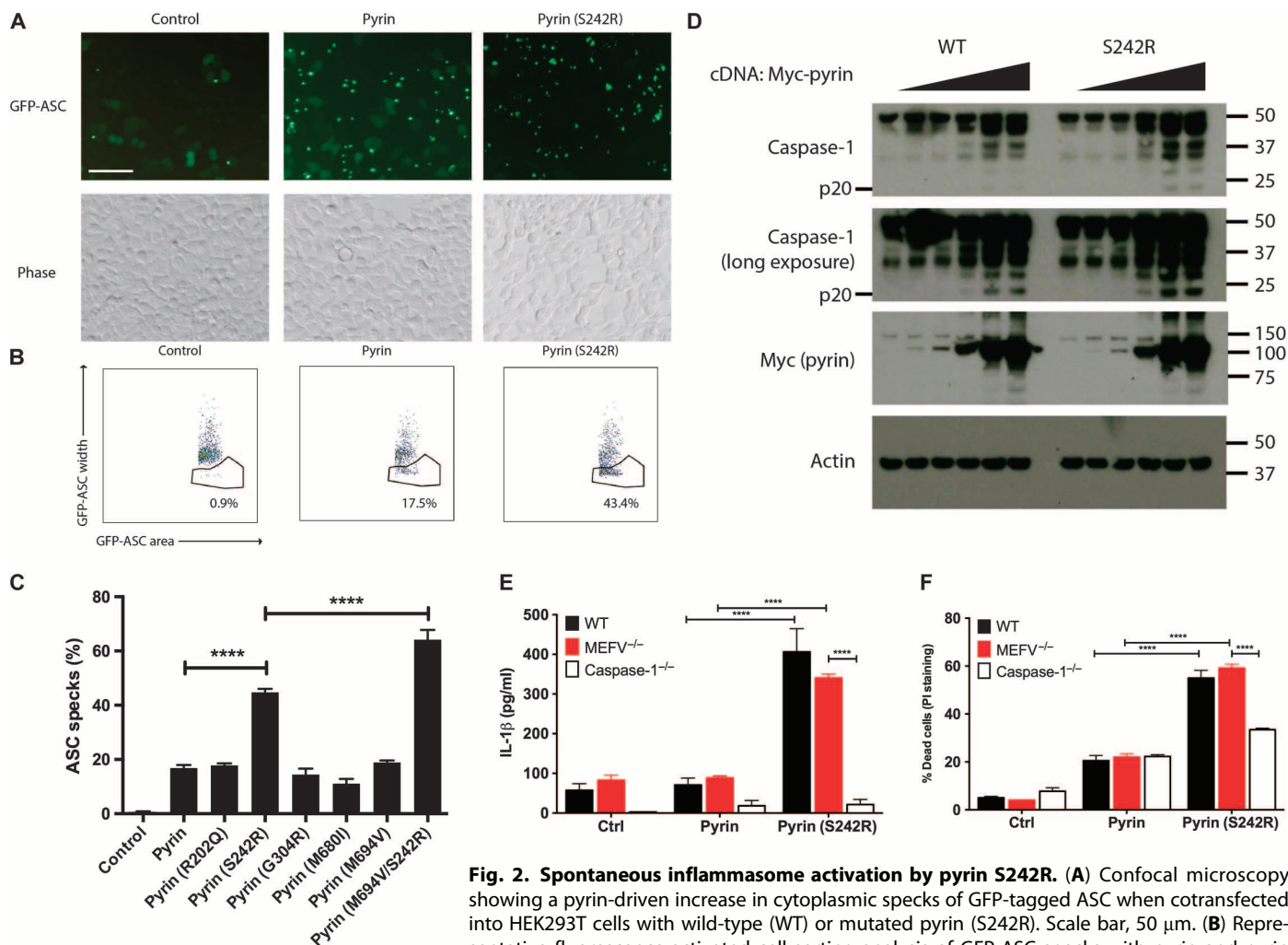


Fig. 2. Spontaneous inflammasome activation by pyrin S242R. (A) Confocal microscopy showing a pyrin-driven increase in cytoplasmic specks of GFP-tagged ASC when cotransfected into HEK293T cells with wild-type (WT) or mutated pyrin (S242R). Scale bar, 50 μ m. (B) Representative fluorescence-activated cell sorting analysis of GFP-ASC specks with pyrin and pyrin S242R. (C) Quantification of three biological replicates for GFP-ASC specks by flow cytometry, with different pyrin mutants. (D) Western blots for active caspase-1 (p20 subunit) after expression of caspase-1 and ASC in HEK293T cells, together with an increasing concentration of Myc-tagged pyrin or pyrin (S242R). cDNA, complementary DNA. (E and F) Monocytic THP-1 cells where caspase-1 or pyrin was deleted by CRISPR, then reconstituted by retroviral expression of pyrin or pyrin (S242R). IL-1 β was measured by enzyme-linked immunosorbent assay (ELISA) (E), and cell death was quantified by propidium iodide (PI) staining and flow cytometry 24 hours after stimulation with LPS (F). All are representative of at least three biologically independent experiments. Error bars represent means + SD for three biological replicates. **** $P < 0.0001$. Ctrl, control.

spectrometry (MS) analysis identified this band as containing the protein 14-3-3 (six of seven human isoforms; fig. S7B). This interaction was then confirmed directly by Western blot, using a pan-14-3-3 antibody (Fig. 3A). Previously, two isoforms of 14-3-3 [epsilon (ϵ) and tau (τ)] were observed to interact with pyrin, dependent on phosphorylation of S242 and S208 (14). In agreement with this, we could observe the phosphorylation of S242 in wild-type pyrin by MS (fig. S7C). Recently, bacterial effectors that target Rho guanosine triphosphatases (GTPases), such as *Clostridium difficile* toxin B (TcdB), were reported to trigger pyrin activation (15). We therefore tested whether their mechanism of action was similar to the S242R mutation, by releasing the inhibitory 14-3-3 protein, and this was indeed the case (Fig. 3B). To confirm the phosphorylation status of S242, we used an antibody that recognizes the pSer 14-3-3 consensus motif (R/K x x pS x P, where x is any amino acid). Although the motif surrounding S242 lacks the +2 proline, the antibody did detect a serine-phosphorylated form of pyrin, and this

was destroyed by the S242R mutation (Fig. 3C and fig. S7D). TcdB treatment also has the same effect, because the pSer 14-3-3 motif in pyrin can no longer be observed after TcdB exposure (Fig. 3C). Together, these data reveal that nonphosphorylated S242, and removal of 14-3-3, is the mechanism by which inhibition of Rho GTPases and the S242R mutation both activate the innate immune receptor pyrin.

In contrast to the PAAND mutation, we found that FMF mutations M680I, M694V, and V726A had no appreciable effect on 14-3-3 binding or the pSer 14-3-3 motif in pyrin (fig. S8A). Moreover, we made a double-mutant pyrin, S208A/S242R, which cannot be phosphorylated at either proposed 14-3-3 binding site, and the FMF mutation M694V was still able to further enhance inflammasome activation (fig. S8B). Therefore, FMF mutations are likely to affect pyrin activity via a mechanism separate from 14-3-3 binding, such as a structural rearrangement in the protein that facilitates inflammasome formation after pyrin activation, allowing FMF mutations to enhance disease presentation (fig. S4B)

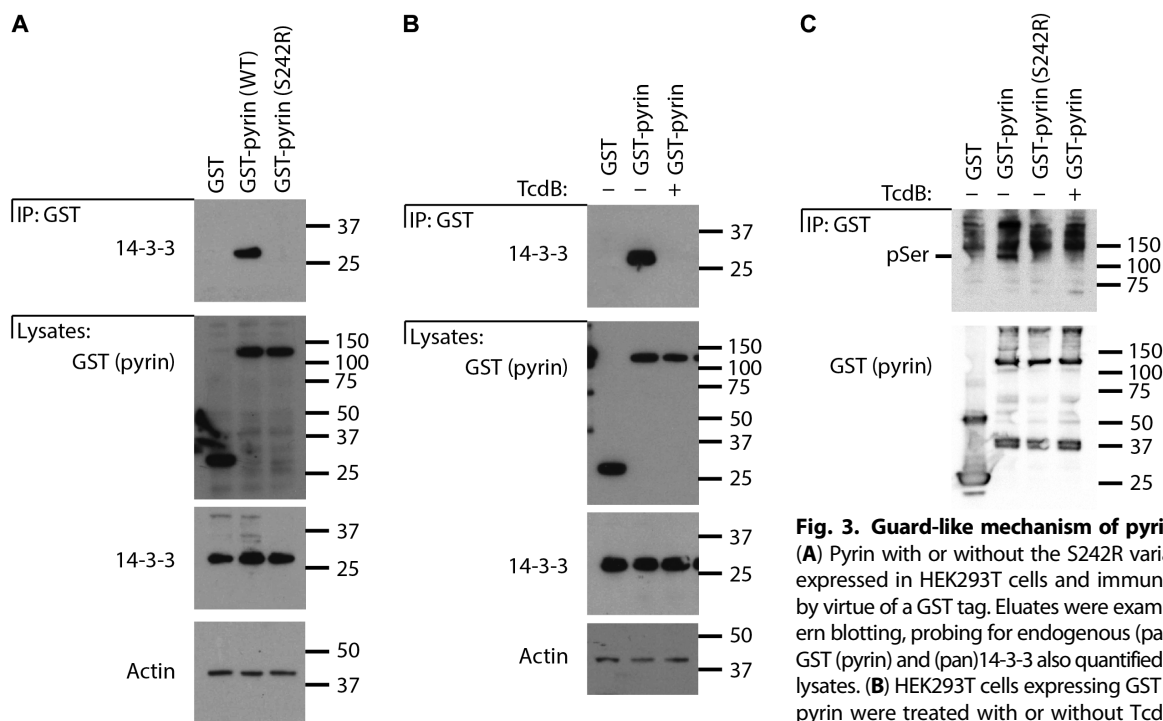


Fig. 3. Guard-like mechanism of pyrin activation.

(A) Pyrin with or without the S242R variant was over-expressed in HEK293T cells and immunoprecipitated by virtue of a GST tag. Eluates were examined by Western blotting, probing for endogenous (pan)14-3-3, with GST (pyrin) and (pan)14-3-3 also quantified in the starting lysates. (B) HEK293T cells expressing GST alone or GST-pyrin were treated with or without TcdB for 6 hours before lysis and analyzed as in (A). (C) HEK293T cells

expressing GST-tagged pyrin or S242R pyrin were left untreated or treated with TcdB as in (B), then immunoprecipitated before Western blotting for pSer (14-3-3 motif) and GST (pyrin). All are representative of at least three biologically independent experiments. IP, immunoprecipitation.

and ASC speck formation (Fig. 2C). Notably, the effect of S208 mutation on enhanced inflammasome activation was minor compared to S242R mutation, indicating a functional hierarchy of importance between these two phosphorylation sites (fig. S8B).

These functional studies suggest that the S242R mutation drives disease in patients by removing the 14-3-3 guard from pyrin, allowing excessive IL-1 β production. To determine whether this process occurred in PAAND patients, we assessed mature IL-1 β production by patient monocytes. Monocytes from healthy individuals did not produce significantly increased levels of mature IL-1 β in response to a short duration of LPS treatment (Fig. 4A) because of the requirement of a second signal for inflammasome activation to allow cleavage of pro-IL-1 β into the mature secreted form. The treatment of monocytes from healthy individuals with both LPS, to induce pro-IL-1 β production, and TcdB, to activate pyrin and thus the inflammasome, resulted in high levels of mature IL-1 β secretion (Fig. 4A). By contrast, patient monocytes demonstrated increased spontaneous inflammasome activation, because LPS alone was sufficient to induce a moderate level of mature IL-1 β (Fig. 4A). No significant difference in IL-1 β secretion was observed between healthy and patient monocytes after TcdB addition alone, indicating similar maximal activities between the dephosphorylated wild-type allele and the S242R allele (Fig. 4A).

The dermal manifestations and relatively modest systemic up-regulation of IL-1 β (Fig. 1) suggested that the process of excessive IL-1 β secretion may be elevated predominantly in the tissues. In support of this, immunofluorescence analysis demonstrated elevated levels of cleaved (active) caspase-1 and mature IL-1 β in skin biopsies from patients with PAAND, whereas levels of pro-IL-1 β remained normal (Fig. 4B). Finally, the central role of this process in the pathogenesis of PAAND was tested through a

clinical trial with anakinra (recombinant IL-1Ra). One of the patients from the UK (G1) was treated with anakinra, after she failed a course of corticosteroids and methotrexate. Shortly after starting anakinra (100 mg daily), her clinical symptoms resolved and, for the first time after several years during which her inflammatory markers were regularly measured, her CRP levels dropped to within normal limits (<5 mg/ml) (Fig. 4C). These observations confirm that the consequences of constitutive pyrin inflammasome activation in PAAND are mediated by IL-1 β and may be effectively controlled using IL-1 β antagonism.

DISCUSSION

The identification of a dominantly inherited autoinflammatory disease with severe neutrophilic dermatosis driven by pyrin S242R mutation greatly expands the spectrum of pyrin inflammasome-related disorders. We propose PAAND as a distinct entity to FMF, due to differences both in clinical phenotype (with distinct characteristic features) and in the underlying molecular mechanism. The clinical presentation of distinct autoinflammatory diseases (FMF and PAAND) from different mutations in the same gene is reminiscent of the effect of *NLRP3* mutation. *NLRP3* mutations are associated with a spectrum of autoinflammatory diseases, including familial cold autoinflammatory syndrome, Muckle-Wells syndrome, and neonatal-onset multisystem inflammatory disease. Although distinct mutations are reportedly associated with each distinct clinical manifestation, a significant overlap is observed.

Our data suggest that clinical presentation of MEFV mutation segregates into clinical phenotype based on the molecular impact of mutation, with defective 14-3-3 binding resulting in PAAND, whereas

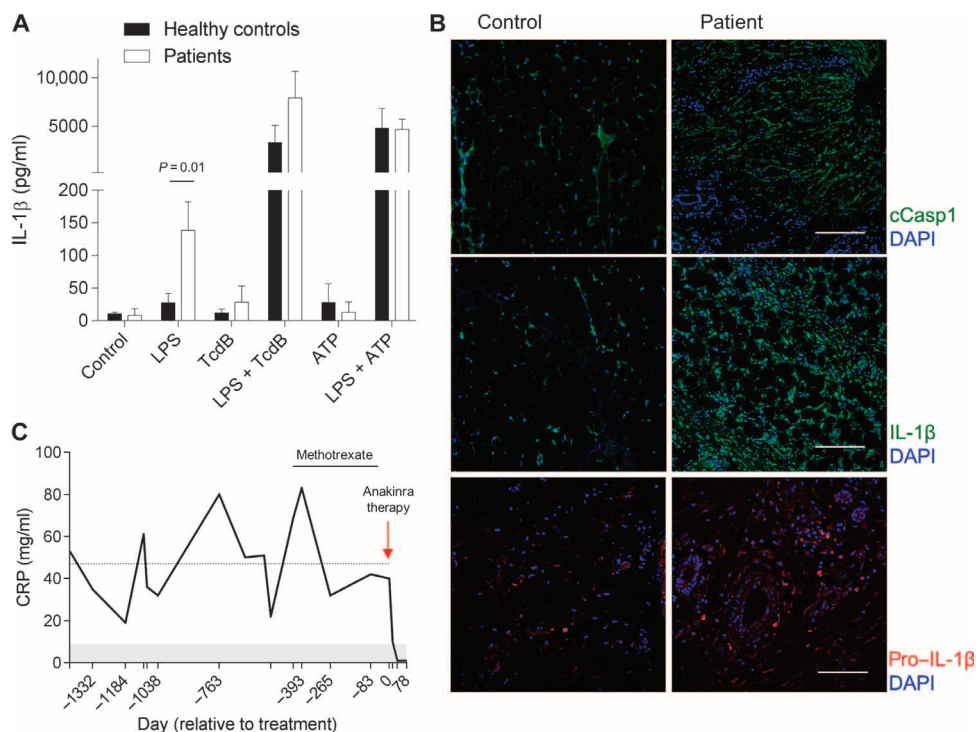


Fig. 4. PAAND is driven by local inflammasome activation and IL-1 β production. (A) Monocytes were purified from three PAAND patients and three healthy controls before stimulation for 1 hour with LPS \pm adenosine triphosphate (ATP), or \pm TcdB. Mature IL-1 β was measured in the supernatant. Means \pm SD for $n = 3$. (B) Immunofluorescence staining for cleaved caspase-1, IL-1 β , and pro-IL-1 β in healthy control skin and an affected biopsy from patient Ill.3 (scale bars, 200 μ m). DAPI, 4',6-diamidino-2-phenylindole. (C) CRP levels were measured before and after treatment with anakinra (100 mg/day) (day 0) in UK patient G1. Dashed line indicates 3-year average CRP level before treatment, arrow indicates initiation of treatment, ticks indicate sample points, and gray zone indicates normal CRP range.

gain-of-function variants result in FMF. However, there are limitations to this gene-phenotype relationship. First, only 17 S242R individuals were included in this study. Fifteen presented with PAAND; however, the pedigree from Lebanon included one individual with both S242R and M694V, with a phenotype that did not fully replicate all PAAND features, and one individual with no apparent disease. The presence of both S242R and M694V was also previously observed in a Lebanese individual reported to have FMF (16), and again, this patient had aspects of both FMF and PAAND, including severe cutaneous abscesses (17). These observations could represent a degree of incomplete penetrance due to genetic or environmental influences, or it may reflect insufficient clinical testing, because the unaffected individual only self-reported their disease status. The presence of both a PAAND and an FMF allele may also complicate the clinical picture. The clinical features of PAAND appear driven by local IL-1 β production, with antagonism of this pathway proving to be a successful therapy in one patient so far; however, a comprehensive prospective clinical and biological evaluation of anakinra treatment has yet to be performed in PAAND.

Our analysis of the S242R mutation uncovered a novel guard-like mechanism by which pyrin is regulated, with loss of S242 phosphorylation licensing pyrin for activation and IL-1 β maturation (fig. S8C). Given our results with TcdB, this study suggests that pyrin may sense pathogens through disruption of S242 phosphorylation. As yet, it is unknown whether

TcdB and other pathogen signals inhibit the relevant kinase or activate a specific phosphatase; however, the net effect is the release of the endogenous inhibitor of pyrin and the subsequent activation of the inflammasome. It is also conceivable that alterations in actin polymerization that trigger pyrin activation (18) may also target S242 phosphorylation or otherwise prevent 14-3-3 binding. Ancestrally, the phosphorylation and constitutive inhibition that we observed for pyrin was first predicated in the guard hypothesis of plant innate immune defense (19), and 14-3-3 homologs have been observed to regulate phosphorylated plant resistance proteins (20). However, in the case of human pyrin activation, the guard (14-3-3) itself is not phosphorylated, so this is an indirect guard-like mechanism, reliant on sensing the balance of the relevant kinase and/or phosphatase downstream of Rho GTPase activity. Similar indirect phosphorylation events regulate plant Nod-like receptor (NLR) activation (21, 22). Phosphorylation may therefore more broadly negatively regulate other mammalian innate immune receptors such as NLRP3, where a mechanism of activation has, to date, proven elusive. In summary, our characterization of a novel autoinflammatory disease, PAAND, identifies constitutive phosphorylation of S242 and the subsequent binding of 14-3-3 as a guard-like mechanism by which pyrin functions as an innate immune sensor of pathogen-mediated disruption of normal phosphorylation processes.

MATERIALS AND METHODS

Human subjects

We documented 22 family members from three generations, all of Flemish (Belgian) ancestry. The family included 12 patients (7 males and 5 females) with a clinical combination of childhood-onset episodes of myalgia/myositis and neutrophilic dermatosis (pyoderma gangrenosum, acne, and cutaneous small-vessel vasculitis), increasing in severity with age. The remaining 10 family members were healthy with no apparent symptoms. Additional pedigrees were included from the UK, France, and Lebanon. Written informed consent was obtained from each participant, and the study was approved by the ethical committee of UZ Leuven (S52653), the Espace Éthique/Université Saint Joseph-Liban, and the Comité de Protection des Personnes Ile de France 5 (Paris, France). Patients from the UK were consented under ethical approval for molecular genetics research studies obtained from South Yorkshire Research Ethics Committee (REC ref. no. 11/H1310/1). Written informed consent to publish images of patients' symptoms was obtained.

Genetic linkage and whole-exome sequence analysis

Whole-genome genotyping for 20 family members (affected and healthy) was performed using the Infinium Human Linkage-12 Genotyping BeadChip (Illumina). The BeadChip includes 6090 common single-nucleotide polymorphism markers with an average spacing of 441 kb and 0.58 cM across the genome. Linkage analysis was performed with the Merlin 1.1.2 software assuming autosomal dominant inheritance, full penetrance, no consanguinity, and a mutation allele frequency of 0.0001. Candidate genes were ranked according to expression in human peripheral blood leukocytes (23).

Whole-exome sequencing was performed for two trios, that is, the proband and both parents. This corresponds to three affected (family members III-3, I-4, II-6, and II-8) and two healthy family members (I-5 and II-9). Genomic DNA samples for whole-exome sequencing were prepared from heparinized peripheral blood using the FlexiGene kit (Qiagen). Exome sequence libraries were prepared using a SeqCap EZ Human Exome Library version 3.0 kit (Roche NimbleGen). Paired-end sequencing was performed on the Illumina HiSeq 2000 (Genomics Core Facility, University of Leuven, Belgium). Alignment of the sequence reads to the Human Reference Genome Build hg19, variant calling, and annotation were done with a pipeline on the basis of BWA (Burrows-Wheeler alignment) (24), GATK (Genome Analysis Toolkit) HaplotypeCaller (25, 26), and Annovar (27). The samples sequenced had an average of 98.2 (range, 57.7 to 127.8) million reads with 93% (range, 87.2 to 94.3) to 81% (range, 57.1 to 88.8) of targeted bases being covered at ≥ 10 - or 30-fold, respectively. To select candidate genes, the following variants were considered: (i) compatible with the presumed mode of inheritance, that is, heterozygous in affected individuals and not present in healthy ones; (ii) overlapping a coding exon or within 2 base pairs of a splicing junction; (iii) not synonymous; (iv) not present in genomic duplications; (v) allele frequency ≤ 0.01 in ExAC 65000; and (vi) absent in 1087 unrelated Belgian individuals without the disease. The pyrin variant identified, rs104895178, has merged into rs104895127. The variation was validated by Sanger sequencing of exon 2 on ABI 3730 XL Genetic Analyzer (Applied Biosystems). Sequencing data were analyzed using the Staden package software.

Cytokine analysis

Plasma samples collected from patients and controls were stored at -80°C . Cytokine levels in plasma were quantified by an electrochemiluminescence immunoassay format using Meso Scale Discovery plates according to the manufacturer's instructions. Data were analyzed with Discovery Workbench 4.0. Plasma IL-1Ra levels were measured using a human IL-1Ra ELISA (Thermo Fisher Scientific) according to the manufacturer's instructions.

Monocytes were isolated from peripheral blood mononuclear cells of patients and controls using CD14 MicroBeads (Miltenyi Biotec) and cultured overnight. The next day, the cells were primed with UltraPure LPS (200 ng/ml) (InvivoGen) for 1 hour before addition of TcdB (1 $\mu\text{g}/\text{ml}$) (Abcam) or 5 mM ATP (InvivoGen). Supernatants were collected after 1 hour and IL-1 β levels were measured by ELISA (R&D Systems).

Cell culture

HEK293T cells were transfected using Lipofectamine (Life Technologies) according to the manufacturer's instructions, using constructs for human Myc-, mCherry-, or GST-pyrin (28), Myc- or GFP-ASC (12), Myc- or GFP-caspase-1 (29), or HA (hemagglutinin)-14-3-3 ϵ (Addgene). *MEFV* mutations were created by site-directed mutagenesis using the

QuikChange Lightning Multi Site-Directed Mutagenesis Kit (Agilent). The *CASPI* knockout THP-1 cells, techniques for lentivirus production, and CRISPR/Cas9-based knockout have been previously described (30). *MEFV*-specific single-guide RNAs (sgRNAs) (exon 1, GGCGTACTCTTCCCCATAGT; exon 2, TCTAGGTCGCATCTTTCCCG) were ligated into the Bsm BI restriction site on the doxycycline-inducible sgRNA vector. Complementation was performed using retrovirus expressing *MEFV* complementary DNA from a pLNCX2 backbone (28). To activate pyrin and induce IL-1 β production and pyroptosis in vitro, THP-1 cells were primed with UltraPure *E. coli* EH100 (Ra) LPS (200 ng/ml) (Enzo Life Sciences) for 30 min before addition of 200 nM TcdB. Cells were incubated for 20 hours before measuring IL-1 β release by ELISA (R&D Systems) and cell death by propidium iodide (Sigma-Aldrich) staining at 1 $\mu\text{g}/\text{ml}$ and flow cytometry. All cell lines were originally from the American Type Culture Collection and tested for mycoplasma contamination.

Western blotting and immunoprecipitation

For Western blotting, THP-1 monocytes were lysed in radioimmunoprecipitation assay buffer or supernatants were concentrated by methanol/chloroform; for immunoprecipitation, HEK293T cells were lysed in NP-40 lysis buffer supplemented with a protease inhibitor (cOmplete protease inhibitor cocktail, Roche). Immunoprecipitation was performed using Glutathione Sepharose 4B (GE Healthcare), with samples eluted in SDS-reducing sample buffer. Eluates were run on SDS polyacrylamide gels and treated as below for MS, or routine Western blotting was performed using the following antibodies: pyrin (Adipogen, rabbit α -pyrin, AL196), caspase-1 (Adipogen, mouse α -caspase-1 p20, Casper-1), IL-1 β (R&D Systems, goat anti-IL-1 β , AB-401-NA), GST (mouse α -GST, in-house), HA (Covance, mouse α -HA1.1), 14-3-3 (Santa Cruz Biotechnology, goat α -14-3-3, sc-629-G), actin (Santa Cruz Biotechnology, goat α -actin, sc-1616), and pSer (Cell Signaling, mouse α -pSer 14-3-3 binding motif, no. 9601). Full Western blots are presented as fig. S9.

MS analysis

Samples were run on SDS polyacrylamide gels, stained using Sypro Ruby (Bio-Rad) and subsequently Coomassie G-250. Bands of interest were excised and subjected to reduction, alkylation, and LysargiNase (31) digestion before MS analysis essentially as previously described (32). Raw files consisting of high-resolution MS/MS spectra were processed with MaxQuant (version 1.5.2.8). Extracted peak lists were searched against the human protein sequences obtained from the UniProt, Swiss-Prot, and Ensembl knowledge bases. Cleavage specificity was set using [X]K/R as a simple cleavage site rule for LysargiNase, allowing up to three missed cleavages.

Fluorescence microscopy and cytometry

GFP-ASC specks and caspase-1 were imaged in HEK293T cells using an Olympus IX70 inverted microscope with 20 \times objective. ASC specks were quantified by flow cytometry (33). In brief, cells gated based on viability and moderate mCherry (pyrin) expression were then selected for calculation of the percentage of cells containing an ASC speck defined by GFP-width versus GFP-area profiles. For colocalization, HEK293T cells were plated on chamber μ -slides (ibidi) and transfected with mCherry-pyrin constructs and ASC-GFP. Images were acquired with a Zeiss LSM 780 confocal microscope, using a 40 \times oil objective. Image channels were merged and converted to TIFF using Fiji software. Immunofluorescence was performed on skin sections fixed in 10%

neutral formalin, embedded in paraffin, and antigen-retrieved with pH 9.0 tris. Sections were blocked and stained with rabbit anti-IL-1 (ab2105, Abcam), IL-1 propeptide (615417, R&D Systems), and rabbit anti-cleaved caspase-1 (4199, Cell Signaling) before developing with donkey anti-rabbit 488 (A-21206, Life Technologies), goat anti-mouse immunoglobulin G1 546, and DAPI (D1306, Life Technologies). Sections were mounted and cover-slipped using Fluoromount-G (SouthernBiotech) before images were acquired with an LSM 510 Meta confocal microscope (Zeiss).

Statistical analysis

Sample sizes were limited by patient availability and are listed in figure legends for each assay. Statistical tests used are detailed in the figure legends. CRP was selected as the outcome of anakinra trial, as the only quantitative measure of inflammation with historical data available from the patient.

SUPPLEMENTARY MATERIALS

www.sciencetranslationalmedicine.org/cgi/content/full/8/332/332ra45/DC1

Fig. S1. Inflammatory manifestations of PAAND.

Fig. S2. Results from linkage analysis.

Fig. S3. Dominant inheritance of PAAND caused by mutation in pyrin, S242R.

Fig. S4. Inheritance of S242R mutations in additional pedigrees.

Fig. S5. Fluorescent microscopy of pyrin/ASC specks.

Fig. S6. Activation of caspase-1 and IL-1 β by pyrin S242R.

Fig. S7. Proteomic analysis of pyrin interactions and phosphorylation.

Fig. S8. Functional effect of FMF mutations in context of pyrin S242R.

Fig. S9. Full Western blots.

Source data (Excel files)

REFERENCES AND NOTES

1. S. L. Masters, A. Simon, I. Aksentijevich, D. L. Kastner, Horror autoinflammaticus: The molecular pathophysiology of autoinflammatory disease. *Annu. Rev. Immunol.* **27**, 621–668 (2009).
2. S. Federici, M. P. Sormani, S. Ozen, H. J. Lachmann, G. Amaryan, P. Woo, I. Koné-Paut, N. Dewarrrat, L. Cantarini, A. Insalaco, Y. Uziel, D. Rigante, P. Quartier, E. Demirkaya, T. Herlin, A. Meini, G. Fabio, T. Kallinich, S. Martino, A. Y. Butbul, A. Olivieri, J. Kuemmerle-Deschner, B. Neven, A. Simon, H. Ozdogan, I. Touitou, J. Frenkel, M. Hofer, A. Martini, N. Ruperto, M. Gattorno, Paediatric Rheumatology International Trials Organisation (PRINTO) and Eurofever Project, Evidence-based provisional clinical classification criteria for autoinflammatory periodic fevers. *Ann. Rheum. Dis.* **74**, 799–805 (2015).
3. French FMF Consortium, A candidate gene for familial Mediterranean fever. *Nat. Genet.* **17**, 25–31 (1997).
4. The International FMF Consortium, Ancient missense mutations in a new member of the *RoRet* gene family are likely to cause familial Mediterranean fever. *Cell* **90**, 797–807 (1997).
5. J. J. Chae, Y.-H. Cho, G.-S. Lee, J. Cheng, P. P. Liu, L. Feigenbaum, S. I. Katz, D. L. Kastner, Gain-of-function pyrin mutations induce NLRP3 protein-independent interleukin-1 β activation and severe autoinflammation in mice. *Immunity* **34**, 755–768 (2011).
6. A. Aldea, J. M. Campistol, J. I. Arostegui, J. Rius, M. Maso, J. Vives, J. Yagüe, A severe autosomal-dominant periodic inflammatory disorder with renal AA amyloidosis and colchicine resistance associated to the *MEFV* H478Y variant in a Spanish kindred: An unusual familial Mediterranean fever phenotype or another *MEFV*-associated periodic inflammatory disorder? *Am. J. Med. Genet. A* **124A**, 67–73 (2004).
7. D. R. Booth, J. D. Gillmore, H. J. Lachmann, S. E. Booth, A. Bybee, M. Soyutürk, S. Akar, M. B. Pepys, M. Tunca, P. N. Hawkins, The genetic basis of autosomal dominant familial Mediterranean fever. *QJM* **93**, 217–221 (2000).
8. M. Stoffels, A. Szperl, A. Simon, M. G. Netea, T. S. Plantinga, M. van Deuren, S. Kamphuis, H. J. Lachmann, E. Cuppen, W. P. Kloosterman, J. Frenkel, C. C. van Diemen, C. Wijmenga, M. van Gijn, J. W. M. van der Meer, *MEFV* mutations affecting pyrin amino acid 577 cause autosomal dominant autoinflammatory disease. *Ann. Rheum. Dis.* **73**, 455–461 (2014).
9. P. Schaner, N. Richards, A. Wadhwa, I. Aksentijevich, D. Kastner, P. Tucker, D. Gumucio, Episodic evolution of pyrin in primates: Human mutations recapitulate ancestral amino acid states. *Nat. Genet.* **27**, 318–321 (2001).
10. A. Ardehshirdavani, E. Souche, L. Dehaspe, J. Van Houdt, J. R. Vermeesch, Y. Moreau, *NGS-Logistics*: Federated analysis of NGS sequence variants across multiple locations. *Genome Med.* **6**, 71 (2014).
11. I. Touitou, S. Lesage, M. McDermott, L. Cuisset, H. Hoffman, C. Dode, N. Shoham, E. Aganna, J.-P. Hugot, C. Wise, H. Waterham, D. Pugner, J. Demaille, C. Sarrauste de Menthier, Infervers: An evolving mutation database for auto-inflammatory syndromes. *Hum. Mutat.* **24**, 194–198 (2004).
12. A. L. Waite, P. Schaner, C. Hu, N. Richards, B. Balci-Peynircioglu, A. Hong, M. Fox, D. L. Gumucio, Pyrin and ASC co-localize to cellular sites that are rich in polymerizing actin. *Exp. Biol. Med.* **234**, 40–52 (2009).
13. T. Jo, K. Horio, K. Migita, Sweet's syndrome in patients with MDS and *MEFV* mutations. *N. Engl. J. Med.* **372**, 686–688 (2015).
14. I. Jéru, S. Papin, S. L'Hoste, P. Duquesnoy, C. Cazeneuve, J. Camonis, S. Amselem, Interaction of pyrin with 14.3.3 in an isoform-specific and phosphorylation-dependent manner regulates its translocation to the nucleus. *Arthritis Rheum.* **52**, 1848–1857 (2005).
15. H. Xu, J. Yang, W. Gao, L. Li, P. Li, L. Zhang, Y.-N. Gong, X. Peng, J. J. Xi, S. Chen, F. Wang, F. Shao, Innate immune sensing of bacterial modifications of Rho GTPases by the Pyrin inflammasome. *Nature* **513**, 237–241 (2014).
16. H. Wittkowski, M. Frosch, N. Wulffraat, R. Goldbach-Mansky, T. Kallinich, J. Kuemmerle-Deschner, M. C. Frühwald, S. Dassmann, T.-H. Pham, J. Roth, D. Foell, S100A12 is a novel molecular marker differentiating systemic-onset juvenile idiopathic arthritis from other causes of fever of unknown origin. *Arthritis Rheum.* **58**, 3924–3931 (2008).
17. T. Kallinich, personal communication.
18. M. L. Kim, J. J. Chae, Y. H. Park, D. De Nardo, R. A. Stirzaker, H.-J. Ko, H. Tye, L. Cengia, L. DiRago, D. Metcalf, A. W. Roberts, D. L. Kastner, A. M. Lew, D. Lyras, B. T. Kile, B. A. Croker, S. L. Masters, Aberrant actin depolymerization triggers the pyrin inflammasome and autoinflammatory disease that is dependent on IL-18, not IL-1 β . *J. Exp. Med.* **212**, 927–938 (2015).
19. J. L. Dangi, J. D. G. Jones, Plant pathogens and integrated defence responses to infection. *Nature* **411**, 826–833 (2001).
20. R. Lozano-Durán, S. Robatzek, 14-3-3 proteins in plant-pathogen interactions. *Mol. Plant Microbe Interact.* **28**, 511–518 (2015).
21. E.-H. Chung, L. da Cunha, A.-J. Wu, Z. Gao, K. Cherkis, A. J. Afzal, D. Mackey, J. L. Dangi, Specific threonine phosphorylation of a host target by two unrelated type III effectors activates a host innate immune receptor in plants. *Cell Host Microbe* **9**, 125–136 (2011).
22. E.-H. Chung, F. El-Kasmi, Y. He, A. Loehr, J. L. Dangi, A plant phosphoswitch platform repeatedly targeted by type III effector proteins regulates the output of both tiers of plant immune receptors. *Cell Host Microbe* **16**, 484–494 (2014).
23. A. Antanaviciute, C. Daly, L. A. Crinnion, A. F. Markham, C. M. Watson, D. T. Bonthron, I. M. Carr, GeneTIER: Prioritization of candidate disease genes using tissue-specific gene expression profiles. *Bioinformatics* **31**, 2728–2735 (2015).
24. H. Li, R. Durbin, Fast and accurate long-read alignment with Burrows–Wheeler transform. *Bioinformatics* **26**, 589–595 (2010).
25. A. McKenna, M. Hanna, E. Banks, A. Sivachenko, K. Cibulskis, A. Kernytzky, K. Garimella, D. Altshuler, S. Gabriel, M. Daly, M. A. DePristo, The genome analysis toolkit: A MapReduce framework for analyzing next-generation DNA sequencing data. *Genome Res.* **20**, 1297–1303 (2010).
26. G. A. Van der Auwera, M. O. Carneiro, C. Hartl, R. Poplin, G. del Angel, A. Levy-Moonshine, T. Jordan, K. Shakir, D. Roazen, J. Thibault, E. Banks, K. V. Garimella, D. Altshuler, S. Gabriel, M. A. DePristo, From FastQ data to high confidence variant calls: The Genome Analysis Toolkit best practices pipeline. *Curr. Protoc. Bioinformatics* **11**, 11.10.1–11.10.33 (2013).
27. K. Wang, M. Li, H. Hakonarson, ANNOVAR: Functional annotation of genetic variants from high-throughput sequencing data. *Nucleic Acids Res.* **38**, e164 (2010).
28. J. J. Chae, H. D. Komarow, J. Cheng, G. Wood, N. Raben, P. P. Liu, D. L. Kastner, Targeted disruption of pyrin, the FMF protein, causes heightened sensitivity to endotoxin and a defect in macrophage apoptosis. *Mol. Cell* **11**, 591–604 (2003).
29. J. J. Chae, G. Wood, K. Richard, H. Jaffe, N. T. Colburn, S. L. Masters, D. L. Gumucio, N. G. Shoham, D. L. Kastner, The familial Mediterranean fever protein, pyrin, is cleaved by caspase-1 and activates NF- κ B through its N-terminal fragment. *Blood* **112**, 1794–1803 (2008).
30. P. J. Baker, D. Boucher, D. Bierschen, C. Tebartz, P. G. Whitney, D. B. D'Silva, M. C. Tanzer, M. Monteleone, A. A. B. Robertson, M. A. Cooper, S. Alvarez-Diaz, M. J. Herold, S. Bedoui, K. Schroder, S. L. Masters, NLRP3 inflammasome activation downstream of cytoplasmic LPS recognition by both caspase-4 and caspase-5. *Eur. J. Immunol.* **45**, 2918–2926 (2015).
31. P. F. Huesgen, P. F. Lange, L. D. Rogers, N. Solis, U. Eckhard, O. Kleinfeld, T. Goulas, F. X. Gomis-Rüth, C. M. Overall, Lysargininase mirrors trypsin for protein C-terminal and methylation-site identification. *Nat. Methods* **12**, 55–58 (2015).
32. J. M. Hildebrand, M. C. Tanzer, I. S. Lucet, S. N. Young, S. K. Spall, P. Sharma, C. Pierotti, J.-M. Garnier, R. C. J. Dobson, A. I. Webb, A. Tripathydonis, J. J. Babon, M. D. Mulcair, M. J. Scanlon, W. S. Alexander, A. F. Wilks, P. E. Czabotar, G. Lessene, J. M. Murphy, J. Silke, Activation of the pseudokinase MLKL unleashes the four-helix bundle domain to induce membrane localization and necroptotic cell death. *Proc. Natl. Acad. Sci. U.S.A.* **111**, 15072–15077 (2014).

33. D. P. Sester, S. J. Thygesen, V. Sagulenko, P. R. Vajjhala, J. A. Cridland, N. Vitak, K. W. Chen, G. W. Osborne, K. Schroder, K. J. Stacey, A novel flow cytometric method to assess inflammasome formation. *J. Immunol.* **194**, 455–462 (2015).

Acknowledgments: We thank the patient families for participation in this study. We thank J. J. Chae (NIH) and D. Gumucio (University of Michigan) for providing pyrin, ASC, and caspase-1 expression constructs and K. Mallants (KU Leuven) for technical support. We thank I. Touitou (Université de Montpellier, INSERM U844), N. Lucidarme, K. Vandevyvere, P. Wynants, P. De Haes, and R. Westhovens for patient care and clinical information. **Funding:** This work was supported by the ERC Start Grant IMMUNO (to A.L.); Interuniversity Attraction Poles (T-TIME); an F+ Post-doctoral Fellowship from the Research Fund KU Leuven (to V.L.); an FWO (Research Foundation–Flanders) fellowship (L.V.E.); an Australian Research Council Future Fellowship (FT130100361, to K.S.); grants from INSERM and GIS (Groupement d'Intérêt Scientifique)–Institut des Maladies Rares; Victorian State Government Operational Infrastructure Scheme Grant, Project Grant (1057815), and Program Grant (1016647); Independent Research Institute Infrastructure Support Scheme Grant (361646); and fellowship (S.L.M.) from the Australian National Health and Medical Research Council. **Author contributions:** S.A. and C.W. initiated the study. S.L.M., I.J., A.G., S.A., C.W., and A.L. designed and supervised the study. S.L.M., P.J.B., D.D.N., L.F.D., C.L.H., F.M., D. Lyras, A.I.W.,

S.E.N., and K.S. are responsible for biochemical experiments to address the function of pyrin S242R. I.J., V.L., L.V.E., D.A.P., D. Lawless, J.E.G.-P., J.D., E.P., P.-Y.J., R.S., L.D.S., E.v.N., J.R.-P., B.C., E.C., M.M.-H., A.M., A.G., S.S., S.A., C.W., and A.L. are responsible for genetic and pathologic examination of patients. S.L.M., C.W., and A.L. wrote the paper with contributions from all authors. **Competing interests:** The authors declare that they have no competing interests.

Submitted 23 December 2015

Accepted 3 March 2016

Published 30 March 2016

10.1126/scitranslmed.aaf1471

Citation: S. L. Masters, V. Lagou, I. Jéru, P. J. Baker, L. Van Eyck, D. A. Parry, D. Lawless, D. De Nardo, J. E. Garcia-Perez, L. F. Dagley, C. L. Holley, J. Dooley, F. Moghaddas, E. Pasciuto, P.-Y. Jeandel, R. Sciot, D. Lyras, A. I. Webb, S. E. Nicholson, L. De Somer, E. van Nieuwenhove, J. Ruuth-Praz, B. Copin, E. Cochet, M. Medlej-Hashim, A. Megarbane, K. Schroder, S. Savic, A. Goris, S. Amselem, C. Wouters, A. Liston, Familial autoinflammation with neutrophilic dermatosis reveals a regulatory mechanism of pyrin activation. *Sci. Transl. Med.* **8**, 332ra45 (2016).



Familial autoinflammation with neutrophilic dermatosis reveals a regulatory mechanism of pyrin activation

Seth L. Masters, Vasiliki Lagou, Isabelle Jéru, Paul J. Baker, Lien Van Eyck, David A. Parry, Dylan Lawless, Dominic De Nardo, Josselyn E. Garcia-Perez, Laura F. Dagley, Caroline L. Holley, James Dooley, Fiona Moghaddas, Emanuela Pasciuto, Pierre-Yves Jeandel, Raf Sciot, Dena Lyras, Andrew I. Webb, Sandra E. Nicholson, Lien De Somer, Erika van Nieuwenhove, Julia Ruuth-Praz, Bruno Copin, Emmanuelle Cochet, Myrna Medlej-Hashim, Andre Megarbane, Kate Schroder, Sinisa Savic, An Goris, Serge Amselem, Carine Wouters and Adrian Liston (March 30, 2016)

Science Translational Medicine **8** (332), 332ra45. [doi: 10.1126/scitranslmed.aaf1471]

Editor's Summary

Guarding inflammation

The innate immune system is hard-wired to protect people from infection. However, mutations in these protective genes can lead to uncontrolled inflammation, resulting in autoinflammatory disease. Now, Masters *et al.* describe a family with an autoinflammatory disease caused by a previously unreported mutation in pyrin. This mutation disrupts pyrin regulation and mimics the effect of pathogen sensing by pyrin, leading to proinflammatory interleukin-1 β (IL-1 β) production. Indeed, targeting IL-1 β resolved disease in one patient. These data suggest that pyrin is regulated through a guard-like mechanism, which guards against autoinflammation in humans.

The following resources related to this article are available online at <http://stm.sciencemag.org>.
This information is current as of September 27, 2016.

- | | |
|-------------------------------|---|
| Article Tools | Visit the online version of this article to access the personalization and article tools:
http://stm.sciencemag.org/content/8/332/332ra45 |
| Supplemental Materials | " <i>Supplementary Materials</i> "
http://stm.sciencemag.org/content/suppl/2016/03/28/8.332.332ra45.DC1 |
| Related Content | The editors suggest related resources on <i>Science's</i> sites:
http://stm.sciencemag.org/content/scitransmed/4/120/120ra16.full
http://stm.sciencemag.org/content/scitransmed/3/81/81ps17.full
http://science.sciencemag.org/content/sci/353/6306/1393.full |
| Permissions | Obtain information about reproducing this article:
http://www.sciencemag.org/about/permissions.dtl |

Science Translational Medicine (print ISSN 1946-6234; online ISSN 1946-6242) is published weekly, except the last week in December, by the American Association for the Advancement of Science, 1200 New York Avenue, NW, Washington, DC 20005. Copyright 2016 by the American Association for the Advancement of Science; all rights reserved. The title *Science Translational Medicine* is a registered trademark of AAAS.